

*Gastrointestinal, Hepatobiliary and Pancreatic Pathology*

# Chronic Alcohol Consumption Accelerates Fibrosis in Response to Cerulein-Induced Pancreatitis in Rats

Xiaoying Deng,\* Lin Wang,<sup>†</sup> Mary S. Elm,\*  
David Gabazadeh,\* Greg J. Diorio,\*  
Patricia K. Eagon,\*<sup>‡</sup> and David C. Whitcomb\*<sup>‡</sup>

From the Department of Medicine,\* Division of Gastroenterology, Hepatology, and Nutrition, University of Pittsburgh, Pittsburgh, Pennsylvania; the Department of Pediatrics,<sup>†</sup> Children's Hospital of Pittsburgh, Pittsburgh, Pennsylvania; the Veteran's Administration Health System of Pittsburgh,<sup>‡</sup> Pittsburgh, Pennsylvania

**Alcohol consumption is a risk factor for chronic pancreatitis (CP), but the mechanism in humans remains obscure because prolonged alcohol consumption in most humans and animal models fails to produce alcoholic chronic pancreatitis (ACP). We hypothesize that the process leading to ACP is triggered by a sentinel acute pancreatitis (AP) event; this event causes recruitment of inflammatory cells, which initiates fibrosis driven by the anti-inflammatory response to recurrent AP and/or chronic oxidative stress. The aim was to determine whether chronic alcohol consumption accelerates fibrosis in response to cerulein-induced pancreatitis in the rat. Wistar male rats were pair-fed control (C) or 5% ethanol (E) Lieber-DeCarli liquid diets. Animals were studied without pancreatitis (P0), with cerulein pancreatitis induced once (P1), or with cerulein-induced pancreatitis weekly for 3 weeks (P3). AP markers, inflammation, and fibrosis were measured histologically, by gene expression profiling and protein expression. Macrophage infiltration was reduced in EP0 versus CP0 rats, but the pattern was reversed after AP. Microabscess, severe necrosis, and early calcification were only induced in the EP3 rats. Fibrosis was significantly induced in the EP3 rats versus EP1, CP1, and CP3 by histology, hydroxyproline content, and mRNA expression for *collagen α1(1)* and *procollagen α2(1)*. Proinflammatory cytokine mRNAs were up-regulated shortly after induction of AP, while the anti-inflammatory cytokines (*interleukin-10* and *transforming growth factor-β*) were strongly up-regulated later and in parallel with fibrogenesis, especially in the EP3 rats. Pancreatic**

**fibrosis develops after repeated episodes of AP and is potentiated by alcohol. Expression of fibrosis-associated genes was associated with expression of anti-inflammatory cytokines in alcohol-fed rats. (*Am J Pathol* 2005, 166:93–106)**

Chronic alcohol consumption is a risk factor for chronic pancreatitis (CP) and is reported to be associated with CP in 50 to 70% of patients.<sup>1</sup> Chronic alcohol consumption alone does not cause alcoholic chronic pancreatitis (ACP) because a small minority of heavy, chronic alcohol drinkers develop clinically recognized CP.<sup>2</sup> The mechanisms linking alcohol consumption to CP are complex and poorly understood, especially because sufficient animal models were previously not available.<sup>3</sup> The fundamental pathological alterations seen in ACP include inflammation and fibrosis with progressive loss of normal parenchyma.<sup>1</sup> Several pathogenic and mechanistic hypotheses for the origin of ACP have been proposed,<sup>1,4–7</sup> but remain either unproven or inadequate in explaining the clinical features.

Recurrent acute pancreatitis (RAP) appears to precede the development of CP in some humans.<sup>8</sup> In chronic alcoholics with CP, approximately two-thirds previously developed RAP 1 to 19 years before development of pancreatic calcification and fibrosis.<sup>9,10</sup> The most compelling clinical evidence that RAP leads to CP comes from patients with hereditary pancreatitis who often have gain-of-function mutations in the cationic trypsin gene (*PRSS1*).<sup>11,12</sup> Loss of trypsin regulation leads to acute pancreatitis (AP), RAP, and finally to CP with all of the pathological features of ACP.

---

Supported by the Veteran's Administration (merit review awards to D.C.W., P.K.E.) and the National Institutes of Health (grant R01 AA10855 to D.C.W.).

Current address for D.G. is Huntington Medical Group, PC, Huntington Station, NY.

Accepted for publication October 6, 2004.

Address reprint requests to David C. Whitcomb, M.D., Ph.D., UPMC Presbyterian, Mezzanine Level 2, C-Wing, 200 Lothrop St., Pittsburgh, PA 15213. E-mail: whitcomb@pitt.edu.

Histological examination of pancreatic tissue from patients with CP reveals inflammatory cells and extensive fibrosis. We hypothesize that the process causing a chronic alcoholic individual to begin to develop CP requires an initiating factor such as an attack of AP to recruit inflammatory cells, especially monocytes/macrophages, which then provide the cytokine signals to direct the subsequent inflammatory and healing (scarring) responses, including regulation of pancreatic stellate cells (PSCs).<sup>13</sup> Together, these resident inflammatory cells are likely to play key roles in driving fibrosis and causing the development of CP in both humans and experimental animals.<sup>3,14–18</sup>

In previous experimental animal studies, chronic alcohol exposure at very high ethanol doses induced minimal morphological changes typically seen in ACP patients.<sup>19–21</sup> Even though CP does not develop in alcohol-fed rats, ultrastructure studies have shown significant mitochondrial damage<sup>22</sup> while biochemical analysis has demonstrated ongoing metabolic and oxidative stress. The metabolic stress is likely aggravated by exocrine hypersecretion in response to food and exogenous CCK stimulation seen in animals chronically fed alcohol.<sup>23,24</sup> Rats that are chronically fed alcohol have an increased sensitivity to AP induced by CCK.<sup>25</sup> Cerulein, an amphibian peptide that acts on the CCK receptors, is widely used to elicit AP by hyperstimulation of exocrine pancreas in rats and mice. The pancreatitis induced by cerulein is characterized by edema, increased serum levels of pancreatic enzymes, inflammation, and in some cases, necrosis.<sup>20</sup> A potential link between AP and CP, which is characterized in part by fibrosis, has been seen in mice with repeated administration of cerulein plus infusion of transforming growth factor (TGF)- $\beta$ .<sup>26</sup>

Based on the above observations, we hypothesize that development of CP requires 1) susceptibility factors for AP; 2) an initiating factor to activate the immune system, and 3) progression factors that drive the pro- and anti-inflammatory systems toward acinar cell destruction and fibrosis. Alcohol could act as factors 1 and 3, but this model would require initiating factors such as AP. Although genetic factors could also play roles such as susceptibility or modifying factors, the fundamental role of alcohol in this process must be demonstrated. Therefore, series of experiments were designed to test the role of alcohol in an animal model of RAP.

## Materials and Methods

### Animals

All animal protocols were approved by the University of Pittsburgh's Institutional Animal Care and Use Committee and the Institutional Animal Care and Use Committee of the VA Medical Center of Pittsburgh. All rats were housed individually in hanging wire cages. The animal room was maintained at 22 to 23°C with lights on from 7 a.m. to 7 p.m.

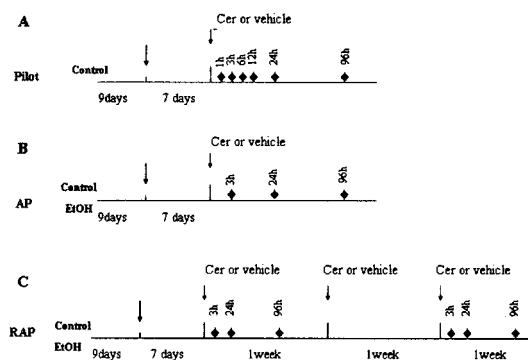


**Figure 1.** Time frame of experimental design. Nine days, ramp time for gradually increasing ethanol concentration in ethanol diet-fed group. Cer, cerulein. ♦, Selected sacrifice time for that group of rats.

### Animal Models

#### Alcohol Models

Male Wistar rats (Harlan Sprague-Dawley, Indianapolis, IN) weighing 200 to 225 g at the beginning of the experiment were allowed to acclimate to the new environment for 1 week with free access to laboratory rat chow (RMH3000; Prolab, St. Louis, MO) and tap water. After 1 week, rats were paired by matching body weights and then fed either an isocaloric control or ethanol-containing liquid diet. The control diet provides 0% and ethanol diet provides 36% of total calories (6.375% v/v) from ethanol, as previously described by Lieber and DeCarli.<sup>27</sup> The ethanol concentration was gradually increased from 0 to 36% of total calories during the first 9 days and the full dose alcohol and control diets were maintained throughout the entire experimental period.

#### Pilot Study (Time Course of Cerulein-Pancreatitis in Control Diet-Fed Rats)

The duration of alcohol feeding needed for rats to adapt physiologically was investigated. Most changes were present by 7 days of full dose of alcohol feeding.<sup>28</sup> To determine an effective time interval for repeated cerulein administration, we studied control-fed rats with a single episode of pancreatitis. After 2 weeks of control liquid diet feeding, rats were given cerulein treatments to induce pancreatitis (Figure 1). Pancreatitis was induced by four hourly intraperitoneal injections of cerulein at the dose of 20  $\mu\text{g}/\text{kg}$  after an overnight fast. Saline injection under the same condition served as a vehicle control. Rats were then sacrificed at 1, 3, 6, 12, 24, 48, and 96 hours after the last injection by an overdose of Nembutal. Blood was collected for measuring serum amylase and ethanol concentration (Sigma Diagnostic alcohol kit, catalogue number 332-B; Sigma, St. Louis, MO), the pancreas was quickly removed, and the wet pancreas weight was measured. A small piece of pancreas was embedded in OCT for morphological studies. The rest was snap-frozen in liquid nitrogen and stored at  $-80^\circ\text{C}$  for RNA and protein extraction.

Peritoneal administration of cerulein at the dose of 20  $\mu\text{g}/\text{kg}$  hourly for 4 hours in the control-fed rats elicited a

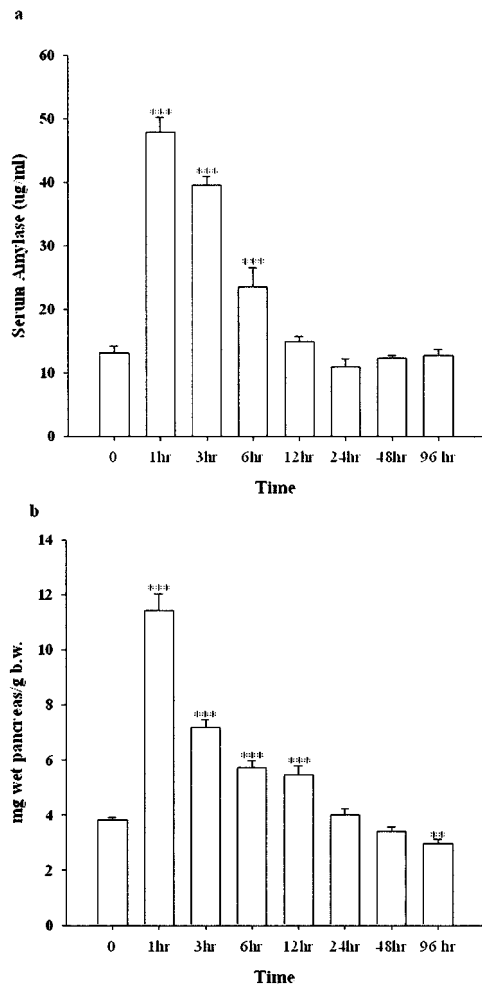


**Figure 2.** The alteration of serum amylase and pancreas wet weight versus body weight induced by cerulein in control-fed rats (pilot study). **a:** Alteration of serum amylase. **b:** Pancreas wet weight versus body weight. \*\*,  $P < 0.01$ ; \*\*\*,  $P < 0.001$ , as compared to the values in the vehicle group.

typical experimental AP. The serum amylase increased as early as 1 hour, and persistently increased at 3 and 6 hours after the final injection. The edema was also developed at 1 hour after the final injection and paralleled the increment of serum amylase (Figure 2a). Quantitatively, the ratio of pancreas wet weight per body weight was significantly increased at the time points of 1, 3, 6, and 12 hours after the last injection as compared to the vehicle-treated rats (Figure 2b). The inflammatory cells, including neutrophils, macrophages, and lymphocytes, began to migrate into the pancreatic parenchyma 3 hours after the final injection (data not shown). At 24 hours, numerous infiltrating cells were already observed in the parenchyma followed by a gradual decline. Therefore, the measurements in subsequent experiments were done at 3, 24, and 96 hours after the final injection of cerulein.

### Experimental Protocols

#### One Episode of Cerulein Pancreatitis (P1)

One week after alcohol-fed rats began to receive a full dose (36%) of ethanol in their diet, cerulein or saline was

administered in these pair-fed rats (control/alcohol) as described above. Rats were sacrificed at 3, 24, and 96 hours after the final injection based on the results of the pilot studies (Figure 1B).

#### Recurrent Acute Pancreatitis (P3)

Rats received the same protocol for cerulein or saline treatment used for P1 except that it was given weekly for 3 weeks. Rats were sacrificed at the same time points after the last cerulein injections as in P1 (Figure 1C).

#### Evaluation of Pancreatitis

The liquid diet intake was monitored daily and the body weight gain throughout the experimental period was measured weekly. The severity of pancreatitis was determined using multiple parameters. Edema was measured by comparing the ratio of the wet weight of the pancreas to rat body weight. The serum amylase levels were measured by the method of Jung.<sup>29</sup> Blood ethanol concentration was measured by using the analyzing kit from Sigma (catalog no: 332B). Histology was done on frozen pancreas samples after they were embedded in the OCT, and sectioned at 10  $\mu\text{m}$  at  $-20^\circ\text{C}$ . Tissue sections were fixed in 10% formalin and stained with hematoxylin and eosin stain. The inflammatory cell infiltration was determined by MPO (myeloperoxidase) stain in whole mount pancreas as previously described,<sup>30</sup> and further characterized by ED2 immunohistochemical stain (1:100; Serotec, Raleigh, NC) and immunoblotting. Collagen deposits in the pancreas were visualized after Gomory's one-step Trichrome stains (Catalog no. HT10-5-16, Sigma) and Sirius Red stain. The quantitative measurement of hydroxyproline in the pancreas was also performed by using the method of Woëssner.<sup>31</sup> To observe the correlation between collagen deposition and inflammatory cells, immunohistochemical detection of  $\alpha$ -smooth muscle cell actin ( $\alpha$ -SMA, marker of PSCs and myofibroblasts,  $\alpha$ -SMA 1:50; DAKO, Carpinteria, CA) or desmin-positive cells (1:100; Santa Cruz Biotechnology, Santa Cruz, CA) as well as immunoblotting were performed. The immunohistochemical stain was performed according to the manufacture's instructions. The visualization of the immunological reactions were performed by using the Vector VIP kit for HRP or Vector Blue kit for ALP (Vector Laboratories, Burlingame, CA). Normal horse/donkey IgG was used as a negative control. Some slides were slightly counterstained with methyl green.

#### Western Blot Analysis

Based on the morphological studies from the pilot experiments, fibrosis was most evident at 96 hours after the last injection of cerulein, and therefore, protein measurements were performed at this time point. Protein was extracted from the pancreas after RNA extraction using Tri reagent (Sigma). The concentration of the purified proteins was measured by using the protein quantification kit (Bio-Rad Inc., Richmond, CA) based on the

method of Lowry and colleagues.<sup>32</sup> Five  $\mu\text{g}$  of protein from each sample was then separated by 7.5, 10.0, or 12.5% sodium dodecyl sulfate-polyacrylamide gel electrophoresis at 120 V using minicell gel apparatus (Bio-Rad Inc.). The separated proteins were then electrophoretically transferred to polyvinylidene difluoride membrane (Immobilon P; Millipore, Bedford, MA) for 30 minutes at 10 V using the semidry transfer module from Bio-Rad Inc. Nonspecific binding was blocked by a 2-hour incubation of the blot in 5% nonfat dry milk in Tris-buffered saline (TBS, pH 7.5). Blots were then incubated overnight with the primary antibodies at 4°C in antibody buffer containing 5% nonfat dry milk in TBST (0.05% v/v Tween 20 in TBS), washed three times with TBST, then incubated for 1 hour with a peroxidase-conjugated secondary antibody in the antibody buffer. After washing, the blots were developed for visualization using an enhanced chemiluminescence detection kit (ECL Western detection system; Amersham, Arlington Heights, IL). The primary antibodies and their titers were as follows: ED 1, 1:500, and ED 2, 1:800, (Serotec Ltd., Kidlington, Oxford, UK) and  $\alpha$ -SMA, 1:200 (DAKO).

#### Determination of Hydroxyproline Level in Pancreas

The content of hydroxyproline in the pancreata were measured according to the method of Woëssner.<sup>31</sup> The level of the hydroxyproline was calculated by using a standard curve from the pure L-hydroxyproline (Sigma) and expressed as ng hydroxyproline per 1  $\mu\text{g}$  of total pancreatic protein.

#### Gene Expression Profile of Pro- and Anti-Inflammatory Cytokines, Extracellular Matrix Markers

##### RNA Extraction

Immediately after rats were sacrificed, total RNA was isolated from pancreas using Tri reagent (Sigma). The extracted RNA was then digested with RNase-free DNase I (Promega, Madison, WI). Integrity of RNA was verified by ethidium bromide staining of rRNA bands on denaturing agarose gel.

##### Gene Expression Profile Defined by Microarray

We evaluated the gene expression profile using the microarray technique. The glass microarray slide, which includes 5535 Oligos (Pan Rat 5K Oligo microarray; MWG-Biotech, Inc., High Point, NC), was hybridized with a probe that was made from the repeated cerulein-treated rats (P3) in the 24-hour groups after the last injection of cerulein according to the manufacturer's instruction. The hybridization signals were analyzed and compared between the EP3 and CP3 group. Twenty  $\mu\text{g}$  of total RNA from five pancreata in the EP3 group (a total of 100  $\mu\text{g}$ ) were pooled to generate the probe for EP3 rats. Likewise, 20  $\mu\text{g}$  of total RNA from five pancreata in the CP3 group were also pooled to generate the probe for

CP3 rats. RNA was then reverse-transcribed into Cy3- or Cy5-labeled cDNA. The RNA was annealed with 1  $\mu\text{g}$  of Oligo d(T<sub>15-20</sub>) primer for 10 minutes at 65°C, then incubated for 2 hours at 39°C with 200  $\mu\text{g}$  of SuperScript II, 5 mmol/L dA/G/TTP, and 1 mmol/L Cy3 (control group) or Cy5 (alcohol-fed group)-labeled dCTP in a 40- $\mu\text{l}$  reaction volume. The labeled cDNA was then purified with Qiagen polymerase chain reaction (PCR) product purification kit (Qiagen, Valencia, CA) and combined as one probe, and applied to the array, covered with a 22-mm<sup>2</sup> glass coverslip, and placed in a sealed chamber. The nonspecific binding was blocked by incubation with 5% bovine serum albumin for 45 minutes at room temperature, followed by hybridization at 42°C overnight. The slides were then washed in three consecutive washes of decreasing ionic strength (2 $\times$ , 1 $\times$ , and 0.5 $\times$  standard saline citrate, 0.1% sodium dodecyl sulfate).

After washing, the slides were scanned at 10- $\mu\text{m}$  resolution to detect Cy3 (control group) and Cy5 (alcohol-fed group) fluorescence by using the microarray scanner from Biodiscovery (model GM18; Biodiscovery Inc., Los Angeles, CA, through the University of Pittsburgh Genomic and Proteomic Core Laboratories). Both Cy3 and Cy5 channels were simultaneously scanned with independent lasers. The area surrounding each element's image was used to calculate a local background that was subtracted from the total element signal (ImaGene version 4.2, Biodiscovery, Inc.). Background-subtracted element signals were used to calculate Cy3: Cy5 ratios. The ratio of the average of the resulting total Cy3 and Cy5 signal were used to normalize or balance the specific signals for each element. Analysis was performed by using Biodiscovery GeneSight software (version 3.0). The reliability of the array experiments was assessed by selection of several genes using real-time quantitative PCR (such as *MCP-1*, *M3*, *collagen  $\alpha$  chain*, *hypoxia-induced factors*, and so forth), and published literature on cerulein-induced pancreatitis or Lieber-DeCarli alcohol-fed rats (such as *CYP2E1*,<sup>33</sup> *heat shock protein*,<sup>34</sup> and so forth), as well as our previous observations.<sup>35-37</sup>

##### Quantization of mRNA Expression by Real-Time Quantitative PCR

Based on the pilot experiments, the altered expression level of RNA was assessed at 3 and 24 hours after the final injection of cerulein. Total RNA (0.5  $\mu\text{g}$ ) was reverse-transcribed according to the manufacturer's recommendations (Invitrogen, Baltimore, MD). RNA was combined with 5  $\mu\text{mol/L}$  random hexamer, 250  $\mu\text{g}$  Superscript II, 40  $\mu\text{g}$  RNase inhibitor (Perkin-Elmer, Foster City, CA), 7.5 mmol/L MgCl<sub>2</sub>, and 1 mmol/L deoxynucleotide triphosphate (dNTP) per 100  $\mu\text{l}$  of reaction volume. The mixture was then cycled through 10 minutes at 25°C, 45 minutes at 48°C, and 5 minutes at 95°C in a thermal cycler. Negative control (no RNA in the reverse transcription) was included in every run of reverse transcription.

The primers were designed using Primer Express software (version 1.5) from Perkin-Elmer Applied Biosystems, Foster City, CA. The efficiency of amplification of the primers was analyzed by separation on 1.2% agarose gel



**Table 1.** Primer Sequences for Real-Time PCR

Primer name	Gene location	Access no.	Sequences (5'—3')	
			Forward	Reverse
18S	557–706	M11188	gag gcc ctg taa ttg gaa tga gtc	tcc caa gat cca act acg agc ttt
Collagen $\alpha$ 1(1)	4179–4245	Z78279	tcg att cac cta cag cac gc	gac tgt ctt gcc cca agt tcc
Fibronectin	3431–3552	NM_019143	cca aag cca ccg gag tct t	ctt gaa gcc aat cct tgg agc
GAPDH	194–263	NM_017008	atg gca cag tca agg ctg aga	cgc tcc tgg aag atg gtg at
HIF-1 $\alpha$	1164–1234	AF057308	tct gag gac acg agc tgc c	gct gga gct agc aga gtc agg
HIF-3 $\alpha$	715–786	AJ277827	ggc ctt tct cag tgg cca c	cca gca act tct gca atc ctc
IL-10	1053–1133	X60675	cca ggt tgc tcc ttc cat ga	cga gac tgg aag tgg ttg cag
IL-12	189–263	S82489	aga tgc tgg cca ata cac ctg	tcc ttc ttg tgg agc agc aga
MCP-1	222–286	M57441	tga gac cag cag cct ttg c	aga tct gcc ggt ttc tct tgg
MIP-1 $\alpha$	126–192	U22414	cga agt ctt ctc agc gcc at	ttg ccg tcc ata gga gaa gc
Procollagen $\alpha$ 2(1)	3636–3699	AF121217	cca acc tgt caa cac ccc a	cca gac atg ctt gtt ggc c
RANTES	167–236	NM031116	gca agt gct cca acc ttg c	ttc tct ggg ttg gca cac ac
TGF- $\beta$ 1	967–1032	NM_021578	gct gct gac ccc cac tga t	cac tgc cgg aca act cca g

and only the primers with a single PCR product were used for further study. The sequences are summarized in Table 1. Gene quantification was performed on the ABI Prism 7700 sequence detection system (Perkin-Elmer Applied Biosystems). Quantitative PCR were performed with SYBR Green core reagent (Perkin-Elmer Bioapplied Biosystems), 2.5  $\mu$ l cDNA products, 250 nmol/L gene-specific primer, 1.25 U AmpliTaq Gold DNA polymerase, 200  $\mu$ mol/L dNTP, as well as 0.5 U AmpErase UNG in a final volume of 25  $\mu$ l. Thermal cycling conditions were as follows: 2 minutes at 50°C, 12 minutes at 95°C, followed by 45 repeats of 15 seconds at 95°C, and 1 minute at 60°C. Each sample was also amplified with 18S and GAPDH primer as an internal control. Data collection was performed during each annealing phase. In each run, a negative control (distilled water), and an RNA sample without the reverse transcription step as well as a negative control for reverse transcription were included. Each reaction was performed in triplicate in a 96-well optical reaction plate (Perkin-Elmer Applied Biosystems). All reactions were performed under the same conditions and the sizes of all amplify reaction from the real-time PCR were rechecked on an agarose gel. Results were analyzed using the ABI sequence detection System (version 1.5) software. All values were normalized to the levels of the housekeeping genes 18S *rRNA*, and expressed as multifold change compared to control liquid diet-fed rats.

**Statistical Analysis**

All data were expressed as the mean  $\pm$  SEM. Each group contained four to seven rats. The comparisons of different

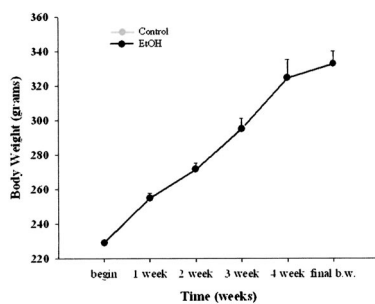


**Figure 3.** Body weight gain throughout the experimental period.

treatments were performed by using analysis of variance and posthoc tests (StatView 4.5; Abacus Concepts Inc., Berkeley, CA). Differences were considered significant at  $P < 0.05$ .

**Results**

A total of 104 Wistar male rats were used for this study. The rats tolerated the Lieber-DeCarli ethanol diet and repeated cerulein treatments with no rats dying during the experiments. The body weight gain in rats fed the ethanol diet with or without cerulein treatment (2.8 to 3.2 g/day) were similar to that in rats fed the chow diets (Figure 3). The average alcohol intake in ethanol-fed alone and ethanol plus cerulein was 12.76 versus 12.91 ml/kg/day of ethanol ( $P > N.S.$ , Figure 4), as previously noted in alcohol-fed alone rats.<sup>38,39</sup> The blood ethanol concentrations fluctuated within the range of 146 to 253 mg/dl.

**Serum Amylase**

The serum amylase was significantly increased at 3 hours after the final injection of cerulein in EP1, CP1, EP3, and CP3 rats (Figure 5). Amylase levels significantly increased in EP3 rats demonstrating active injury ( $P < 0.05$ , note that the lower amylase levels in alcohol-fed rats could also reflect altered expression of the amylase gene compared to protease genes as opposed to less injury).

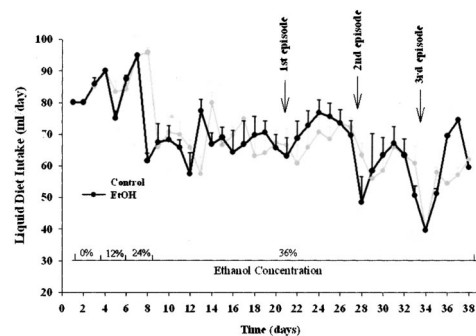


**Figure 4.** The daily average intake of control and alcohol-liquid diets consumed by control-fed and alcohol-fed rats (ml/day/rat). First, second, and third episode, demonstrated the four injections of the cerulein at that specific day.

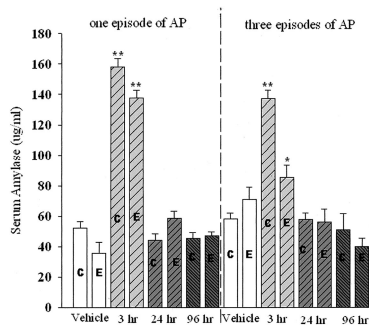


**Figure 5.** Comparison of one episode and three episodes of cerulein pancreatitis on serum amylase levels. C, Control diet-fed rats; E, alcohol liquid diet-fed rats. \*,  $P < 0.05$ ; \*\*,  $P < 0.01$ , as compared to the respective vehicle-treated group.

### Edema

In P1 pancreatic edema in alcohol-fed rats was significantly increased as compared to the vehicle-treated rats in terms of pancreas wet weight per body weight at 3 hours after the final injection ( $P < 0.05$ ). However, the amplitude of the increment is much smaller than that in cerulein-treated control-fed rats (Figure 6). In P3 the repeated cerulein treatments induced only moderate pancreatic edema in both control- and alcohol-fed rats as compared to their corresponding vehicle-treated rats. However, the pancreatic edema was far less severe than that in one-cerulein treatment rats.

### Histology

As illustrated in Figure 7A, no histological change was found in the pancreas of control liquid diet-fed rats with vehicle treatment. Pancreatic pathological changes were minimal in rats fed the ethanol diet alone with vehicle treatment (Figure 7B) after 1 and 4 weeks of feeding as previously reported.<sup>38,40,41</sup> Likewise, there is no difference in terms of extracellular matrix deposition between alcohol versus control liquid diet-fed rats (Figure 7).

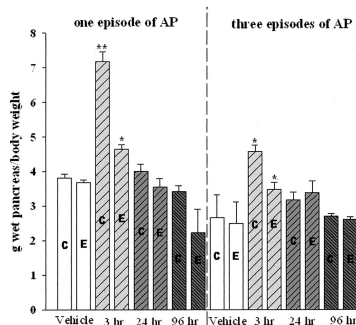


**Figure 6.** Comparison of one episode and three episodes of cerulein pancreatitis on pancreas wet weight versus body weight. C, Control diet-fed rats; E, alcohol-liquid diet-fed rats. \*,  $P < 0.05$ ; \*\*,  $P < 0.01$ , as compared to their corresponding vehicle-treated group (control-fed cerulein/control-fed vehicle, alcohol-fed cerulein/alcohol-fed vehicle).

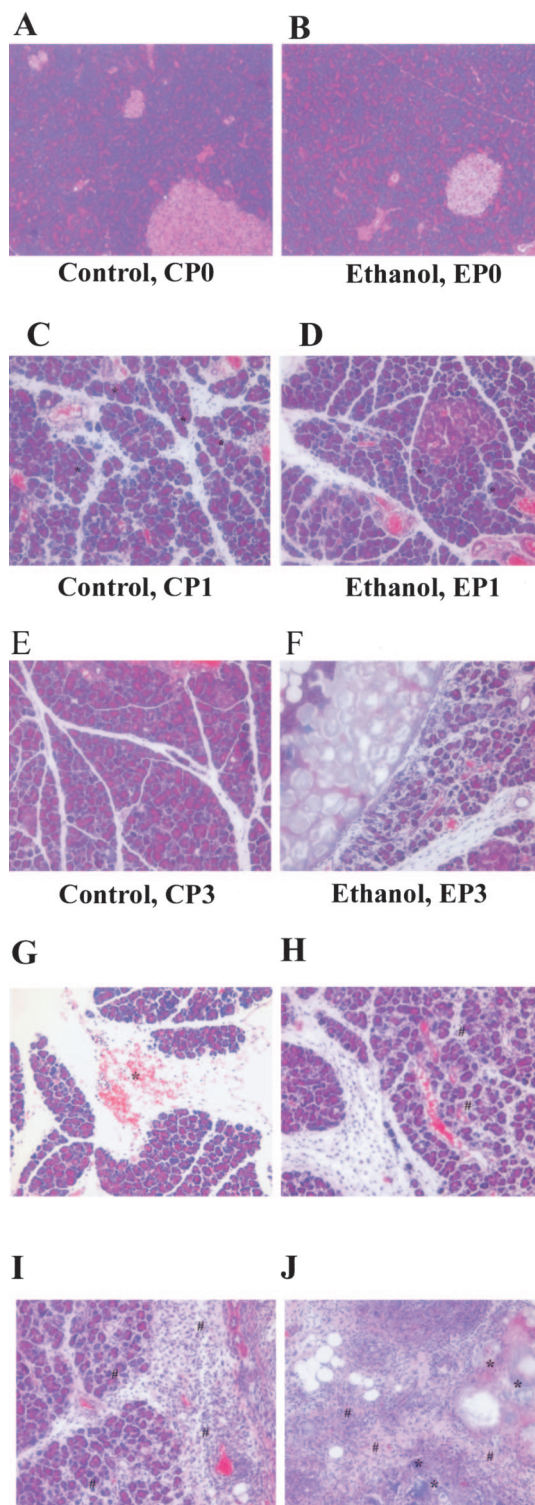


**Figure 7.** Representative pancreatic tissue sections from vehicle-treated control-fed rats (A, CP0); vehicle-treated alcohol-fed rats (B, EP0); 24-hours one episode of cerulein pancreatitis control-fed rats (C, CP1) (\*, typical vacuolization in acinar cells); 24-hours one episode of cerulein pancreatitis alcohol-fed rats (D, EP1) (\*, typical vacuolization in acinar cells); 96-hours three episodes cerulein pancreatitis control-fed rats (E, CP3); 96-hours three episodes cerulein pancreatitis alcohol-fed rats (F, EP3). **G–J:** Findings in EP3 rats. **G:** Hemorrhage (labeled as \*); **H:** white blood cell infiltration (labeled as #) and acinar cell necrosis; **I:** severe white blood cell infiltration around the necrosis and calcification; and **J:** calcification (labeled as \*) and early fibrosis (labeled as #) in parenchyma of pancreas in EP3 rats. H&E stain. Original magnifications,  $\times 200$ .

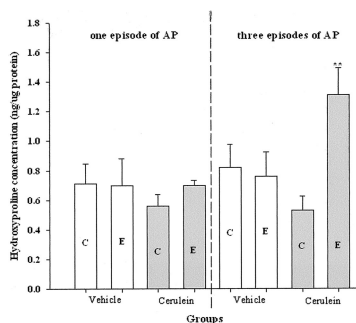


**Figure 8.** The alterations of pancreatic hydroxyproline levels at 96 hours after the last injection in vehicle-treated, one or three episodes cerulein pancreatitis. C, Control-fed group; E, alcohol-fed group. \*\*,  $P < 0.01$ , as compared to the vehicle-treated group.

### P1

A single episode of cerulein pancreatitis did not induce any significant increase in the deposition of extracellular matrix in pancreatic parenchyma (Figure 7C) or pancreatic hydroxyproline level in vehicle- and ethanol-fed rats (Figure 8). However, as demonstrated in Figure 7C, vacuolization was more severe in the pancreata of control-fed rats as compared to alcohol-fed rats (Figure 7D).

### P3

By 96 hours after the last cerulein injection in control rats (CP3), the altered pancreatic structure induced by the repeated cerulein treatments demonstrated rapid recovery, including intralobular septa and pancreatic lobules (Figure 7E). At this time point, the inflammatory cells were resolving and the necrotic acinar cells were replaced by normal acinar cells (Figure 7E). However, in alcohol-fed rats (EP3), patchy and severe inflammation persisted throughout the parenchyma in all rats (Figure 7F). These alterations included hemorrhage, microabscess, and acinar cell necrosis, as well as severe white blood cell infiltration (Figure 7; G to J). Calcification appeared in areas of presumed necrosis with early fibrosis being evident within these areas. Microabscess, severe necrosis, and early calcification were only seen in EP3 rats. The intralobular septa were abnormally expanded and with occasional pancreatic lobules split. Sirius Red staining revealed new connective tissue around the duct system and near acinar cells (Figure 9). Furthermore, pancreatic hydroxyproline level was dramatically increased at 96 hours in alcohol-fed rats (EP3, Figure 8) as compared to CP1, EP1, and CP3 rats. Real-time quantitative PCR revealed significant up-regulation of collagen  $\alpha 1(1)$  and fibronectin in EP3 rats (Table 2 and Figure 10). Western blot analysis also revealed a clear parallel increase of collagen type 1 at protein levels (data not shown).

### Cellular Infiltration

In P1, in contrast to the edema, the inflammatory cell infiltrations into pancreatic parenchyma were more severe in alcohol-fed rats than that in control-fed rats (Figure 11 and Figure 7, H and I). In P3 the inflammation

induced by the repeated cerulein treatment in pancreata in control-fed rats resolved by 96 hours after the last injection. However, inflammation in EP3 rats was more severe than CP3 rats at 24 hours and persisted until 96 hours. ED2-positive cells (resident macrophages) were mainly distributed along the interlobular/intralobular septa and acinar cells within necrotic regions. The increase in ED2 was confirmed with Western immunoblot (Figure 12).

### Pancreatic Stellate Cells

In control-fed rats, the repeated cerulein treatment activated  $\alpha$ -SMA-positive cells in the septa of pancreata during the early period of the inflammation with a peak ~24 hours after the final injection. However, in alcohol-fed rats, numerous  $\alpha$ -SMA-positive cells were still present in the interstitium around acini and necrotic region, intralobular ducts, as well as patched fibrogenetic areas 96 hours after the final injection (Figure 12). The  $\alpha$ -SMA immunoblots further supported this observation (Figure 12).

### Microarray Analysis

Microarray analysis showed that significant alterations of multiple genes were evident in the EP3 rats. As summarized in Table 2, of the 5535 genes that were selected for this microarray, the repeated cerulein treatments up-regulated ~2.98% of the genes more than 10-fold, and 8.1% more than twofold in alcohol-fed rats compared to control rats. Of the genes 0.6% were down-regulated twofold and 1.25% of the genes were more than onefold down-regulated as compared to control rats (Table 2). The genes identified by the microarray technique mainly belong to five different categories: 1) apoptosis; 2) ethanol metabolism and oxidative stress; 3) fibrogenesis and extracellular matrix; 4) chemokines, cytokines, and growth factors; and 5) transcription factors. In addition, one-third of the up-regulated genes have been reported to be associated with the development of cerulein-induced pancreatitis or expressed in liver, pancreas, or other tissues from the Lieber-DeCarli alcohol-fed rats. In particular, genes associated with fibrosis that were up-regulated in EP3 rats included: *troponin I*, *vascular endothelial growth factor D (VEGF-D)*,  *$\alpha 4$  type V collagen*, *fibroblast growth factor 13*, *muscle regulatory factor (MRF4) gene*, *stromelysin 3*, *procollagen C-proteinase enhancer protein*, and some other adhesion molecules, with each increasing 6- to 94-fold, respectively. Other alterations are summarized in Table 2.

### Alterations of Pro- and Anti-Inflammatory Cytokines

Microarray analysis demonstrated that several key cytokines are significantly up-regulated in EP3 ethanol diet-fed rats. This was confirmed by real-time quantitative PCR. The expression levels of the proinflammatory cytokines including *MCP-1*, *MIP-1*, *RANTES*, as well as anti-

**Table 2.** List of the Main Genes Altered by Recurrent Cerulein-Induced Pancreatitis in Chronic Alcohol-Fed Rats

	Cy3/Cy5 signal	Accession No.	Gene names
Apoptosis Up-regulated	498.1	u72349	Bcl-xbeta
	46.9	u34932	Fos-related antigen; FRA
	23.4	u40188	Neuronal cell death-related gene in neuron-7 (DN-7); induced upon programmed cell death in neuronally differentiated PC12 cells
	19.4	u09793	p21 (c-Ki-ras)
	10.3	s76513	bcl-x = apoptosis inhibitor (protooncogene) (ovary, mRNA Partial, 726 (nt); apoptosis inhibitor
	7.7	l41275	p21 protein (cip1) gene
	6.9	af136282	Apoptotic death agonist BID (BID)
	6.3	af243515	BCL2/adenovirus E1B 19 kd-interacting protein 3 (Bnip3); nuclear mitochondrial product; BNIP3; NIP3; pro-apoptotic mitochondrial
	2.9	af222733	DEAD box protein 1 (Ddx1) partial cds
	2.8	u12187	Ras-related protein (rad); ras-related protein
Down-regulated	-3.3	af239739	Death-up-regulated gene (DUG)
	-2.8	ay029163	BCL2L10 (Bcl2l10); Boo, Diva
Cell growth and differentiation Up-regulated	109.7	af002281	Alpha-actinin-2 associated LIM protein; ALP
	99.5	m74295	rhoB gene
	94.3	af271786	Fibroblast growth factor 13 (Fgf13)
	85.9	af036255	RING finger protein; contains B-box, coiled-coil, ABP repeat, B-propeller, WD repeat, RBCC domain
	79.0	l13619	Growth response protein (CL-6); insulin-induced
	63.3	af205717	Tetraspan protein LRTM4 (LRTM4)
	46.0	af172174	Urotensin II precursor
	44.4	x54806	Cytokeratin type I (3' end)
	43.3	s70803	Clone p10.15 product (osteosarcoma ROS17/2.8, 737 (nt);
	38.9	u47673	Sodium-cotransporter rkST1 partial cds; member of the SGLT1-transporter-family
	37.8	j03886	Skeletal muscle myosin light chain kinase; skeletal muscle light chain kinase (E.C. 2.7.1.37)
	34.4	u61748	Clone 9-32 (Rk9-32), dynein heavy chain (Dnchc2) partial cds; overlaps with GenBank accession no. D26495; molecular motor
	33.3	j02713	Mast cell protease-like gene, 5' end; homologue
	32.7	l09120	Calpain II 80 kd subunit
	27.1	af028784	Glial fibrillary acidic proteins alpha and delta (GFAP) gene, alternatively spliced products; intermediate filament; alternatively spliced
	26.4	m84685	Muscle regulatory factor (MRF4) gene
	26.0	af272661	Alpha 4 type V collagen; collagen alpha chain
	24.3	u46034	Stromelysin 3
	22.6	s54212	Ciliary neurotrophic factor receptor alpha component (brain, 1332 (nt))
	22.6	d14014	Cyclin D1
	18.8	af177694	Protocadherin-T2 (pcdh-T2) partial cds; protocadherin gamma family member
	16.3	ab020022	Neuronal differentiation-related; neuronal differentiation-related gene
	16.5	m83177	Amyloid P component (SAP)
	16.3	ab020022	Neuronal differentiation-related; neuronal differentiation-related gene
	12.6	l35271	AML1
	12.2	af014827	Vascular endothelial growth factor D (VEGF-D)
	10.6	u66470	Cell growth regulator rCGR11
	7.8	m76535	Gap junction structural protein, connexin (CXN-40) gene
	6.3	m92074	Troponin I
	5.9	af016503	Procollagen C-proteinase enhancer protein (PCPE)
	5.9	af178086	Kidney-specific membrane protein NX-17
	5.9	d83348	Long-type PB-cadherin
	5.9	u05784	Microtubule-associated proteins 1A and 1B light chain 3 subunit
5.7	af077338	Myosin-binding protein H; MyBP-H	
3.4	af311311	P116RIP; Rho-interacting protein; similar to <i>Mus musculus</i> p116Rip	
Down-regulated	-2.2	af236054	Liver regeneration-related protein 1
	-2.4	af277717	Fibroblast growth factor receptor 3 (Fgfr3)
	-3.7	af324043	Claudin-11; tight junction protein
	-4.0	u11031	Neural cell adhesion molecule BIG-1 protein (BIG-1)
	-588.3	m93005	Guanylin; precursor

(Table continues)



**Table 2.** *Continued*

	Cy3/Cy5 signal	Accession No.	Gene names
Inflammation			
Up-regulated	124.1	af182508	Pre-T cell receptor alpha-type chain partial cds
	64.7	x00336	Interferon-alpha 1 (IFN-alpha1)
	58.8	af286344	Immunoglobulin 4G6 light chain variable region partial cds
	38.8	d87840	Madcam 1
	37.9	m23885	T-cell receptor beta-chain mRNA V-region (V-J-C), clone CRTB29; T-cell receptor beta chain precursor
	32.1	af118854	Immune suppressor factor J6B7-like protein partial cds
	13.9	af113922	MHC class II antigen B beta chain (RT1.Bbeta) gene, partial cds
	13.1	af015718	Interleukin-15 alternative-splice product (IL-15); lacks 16 amino acids compared to normal product
	11.9	aj277828	Hypoxia-inducible factor 2 alpha (Hif-2a gene)
	10.1	m57441	Chemoattractant protein-1 (MCP-1)
	9.7	m87786	(Hybridoma YTH655) immunoglobulin light chain variable region, complementarity-determining regions partial cds; anti-CD2 (T11; LFA-2) variable region; putative
	5.7	af187860	Hsp70-binding protein HspBP; rat HspBP; HspBP1 isoform
	3.4	u90448	CXC chemokine LIX
Down-regulated	-16.2	m87634	BF-1
	-9.9	af091576	Isolate HFL-VN1 olfactory receptor partial cds
	-7.3	d86642	FK506-binding protein 12.6
Metabolism			
Up-regulated	64.0	af038870	Betaine homocysteine methyltransferase (BHMT)
	53.6	l36250	(Clone 71) triosephosphate isomerase
	47.6	l34821	Succinate-semialdehyde dehydrogenase (SSADH) 3' end
	34.9	af061442	Cytochrome P450 2E1
	27.1	k03248	Phosphoenolpyruvate carboxykinase (GTP) gene, exons 9 and 10 and complete cds; phosphoenolpyruvate carboxykinase
	26.9	u23769	CLP36 (clp36)
	25.5	af017393	Cytochrome P4502F4 (CYP4502F4)
	24.9	u02096	Fatty acid binding protein
	24.8	l14284	N-acetylglucosaminyltransferase V
	22.0	af100154	Kynurenine aminotransferase/glutamine transaminase K (Kat) gene
	21.1	u23146	Mitogenic regulation SSeCKS (322) gene; Src suppressed C kinase substrate
	20.4	d00575	Pituitary glycoprotein hormone alpha-subunit precursor
	17.2	u77583	Casein kinase I alpha L (CK1aL)
	16.8	m22631	Alpha-propionyl-CoA carboxylase; alpha-propionyl-CoA carboxylase (EC 6.4.1.3)
	16.3	j05210	ATP citrate-lyase
	16.8	m22631	Alpha-propionyl-CoA carboxylase; alpha-propionyl-CoA carboxylase (EC 6.4.1.3)
	16.3	j05210	ATP citrate-lyase
	12.5	u57042	Adenosine kinase
	9.1	x76988	Gal beta 1,3 galNAc alpha 2,3-sialyltransferase
	8.8	d13121	ATP synthase subunit e
	6.5	m29249	3-Hydroxy-3-methylglutaryl coenzyme A reductase gene, partial cds
	4.8	af006617	Microsomal stress 70 protein ATPase core (Stch); similar to HSP70
	3.8	m88592	Peroxisome proliferator-activated receptor (PPAR)
	3.0	m15893	Pancreatic lysophospholipase; lysophospholipase precursor
	2.8	u39943	Cytochrome P450 monooxygenase (CYP2J3); hemoprotein; arachidonic acid epoxygenase and omega-1 hydroxylase
Down-regulated	-16.7	af163318	Putative N-acetyltransferase Camello 1 (cm11)
	-53.4	s61804	O6-methylguanine-DNA methyltransferase [liver, 812 nt];
	-70.1	m67465	3-beta-hydroxysteroid dehydrogenase/delta-5-delta-4-ene-isomerase; 3-beta- hydroxysteroid
	-107.8	m61112	Delta-3,delta-2-enoyl-CoA isomerase
Transcription factors			
Up-regulated	50.8	af199334	NIM2 (Nim2)
	50.6	l01702	Protein-tyrosine-phosphatase (LRP)
	35.6	u17013	Transcription factor Oct1 (Oct1) partial cds; based on comparisons with Oct1 from other species, this cDNA is probably missing the region encoding 114-115
	20.3	u41845	Nuclear pore complex protein Nup50 (Nup50)
	19.6	af181251	Lung Kruppel-like factor (Lklf) gene; zinc finger transcription factor; similar to mouse LKLF

(Table continues)

**Table 2.** *Continued*

	Cy3/Cy5 signal	Accession No.	Gene names
Signal transduction Up-regulated	14.6	af246634	I-Kappa-B-beta; IκB-b; IκB protein family member; inhibitor of NF-kappa B; may account for persistent activation of NF-kappa B; regulated by
	13.1	aj007467	Putative zinc-finger protein, partial
	6.9	af107843	TATA element modulatory factor; similar to Homo sapiens TATA element modulatory factor
	5.7	u35365	Proto-oncogene FYN (p59fyn)
	5.2	ab003091	IRF-2, partial cds
	4.6	j03823	Mas oncogene; mas oncogene encoded protein
	4.6	u37101	Granulocyte colony-stimulating factor
	4.1	af042499	Smad7; Mad homolog
	3.7	x91810	Stat3 protein; single, polypeptide chain; needs to form homo- or heterodimers for specific DNA-binding
	3.2	u17837	Zinc finger protein RIZ
	37.5	l18948	Intracellular calcium-binding protein (MRP14)
	35.6	af016247	RTK40 homolog (tyro10); tyrosine kinase
	32.9	u16802	Ca <sup>2+</sup> -dependent activator protein (CAPS); similar to <i>C elegans</i> Unc-31; calcium-dependent activator protein for secretion; calcium-dependent
	24.7	l08494	GABA-A receptor alpha-5 subunit gene
	23.7	ab017656	Muscarinic receptor m3
	23.5	d13126	Neural visinin-like Ca <sup>2+</sup> -binding protein type 3 (NVP-3); NVP-3
	22.7	af076619	Molecular adapter rGrb14 (Grb14); signal transduction protein; Grb7 family member; binds the insulin receptor
	20.1	l25264	G-protein-coupled muscarinic potassium channel (GIRK1)
	16.2	af000300	Lyn A tyrosine kinase (LynA); Src-family protein tyrosine kinase
16.2	af000300	Lyn A tyrosine kinase (LynA); Src-family protein tyrosine kinase	
15.0	af001423	N-methyl-D-aspartate receptor NMDAR2A subunit; NMDA receptor NMDAR2A subunit	
Miscellaneous Up-regulated	13.7	af040750	G protein-coupled receptor kinase 6, splice variant C (GRK6); GRK6C
	12.5	af135265	Large-conductance calcium-activated potassium channel (slo); maxi-k channel isoform
	6.2	l08610	Alpha-1B adrenergic receptor gene, exon 2 and complete cds
	5.6	u39875	EF-hand Ca <sup>2+</sup> -binding protein p22
	67.0	u62315	Alpha-globin (GloA) gene; minor gene
	57.9	af135839	Homeodomain protein RX (Rx)
	51.3	af168795	Schlafen-4 (SLFN-4)
	40.8	af227145	Candidate taste receptor T2R8; G protein-coupled receptor
	39.0	m64385	Olfactory protein
	34.4	d37885	Choline kinase R2, partial cds
31.9	ab048823	KCNK3b TASK1 splice bvariant (TASK1b)	

inflammatory cytokines including *TGF-β*, *interleukin (IL)-10*, and *IL-12* are summarized in Table 3.

### Discussion

One of the major limitations in understanding chronic alcoholic pancreatitis has been the lack of an appropriate animal model. We hypothesized that development of most forms of CP required several sequential factors.<sup>42</sup> These factors could be broadly classified as susceptibility factors, initiating factors, and progression factors. The current studies demonstrate that the key features of ACP are reproduced in the rat with chronic alcohol plus RAP. Neither alcohol alone, nor three episodes of recurrent pancreatitis alone are sufficient to cause CP. These findings, when combined with previous studies, are consistent with the hypothesis that alcohol is both a suscepti-

bility factor and a progression factor, but ACP requires an initiation factor, such as an AP event<sup>42</sup> and additional progression factors such as RAP.

The current model allows us to investigate the mechanisms leading to collagen and fibronectin expression and deposition in the EP3 rats. Four major observations were made. First, alcohol feeding alone (EP0) was associated with a marked reduction in immunocytes and evidence of inflammation (Figures 7 and 11). Second, the immune response to an initial episode of AP in the alcohol-fed rats (EP1) was exaggerated compared to controls (CP1), even though the injury was less (see macrophage count and ED2 stain in Figure 11, and proinflammatory cytokine responses of EP1 versus CP1 rats in Table 3, amylase and edema in Figures 5 and 6). Third, the severity of cerulein-induced pancreatic injury was diminished after the initial episode of active pancreatitis (re-

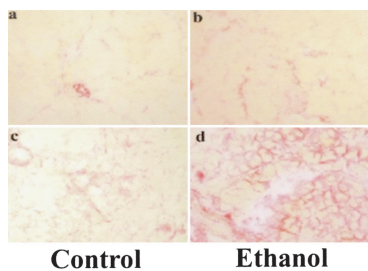


**Figure 9.** Representative tissue sections stained by Sirius Red. **a:** Control vehicle-treated group (CP0); **b:** ethanol vehicle-treated group (EP0); **c:** 96-hours three episodes of cerulein pancreatitis in control-fed group (CP3); and **d:** 96-hours three episodes of cerulein pancreatitis in alcohol-fed group (EP3). Sirius Red stain. Original magnifications,  $\times 100$ .

duced amylase levels and edema in CP3 versus CP1 and EP3 versus EP1, Figures 5 and 6) and was associated with an increase in anti-inflammatory cytokines. Finally, the anti-inflammatory cytokine response, inflammatory cell infiltrate, stellate cell activation, and markers of fibrosis were markedly elevated only in the rats with both RAP

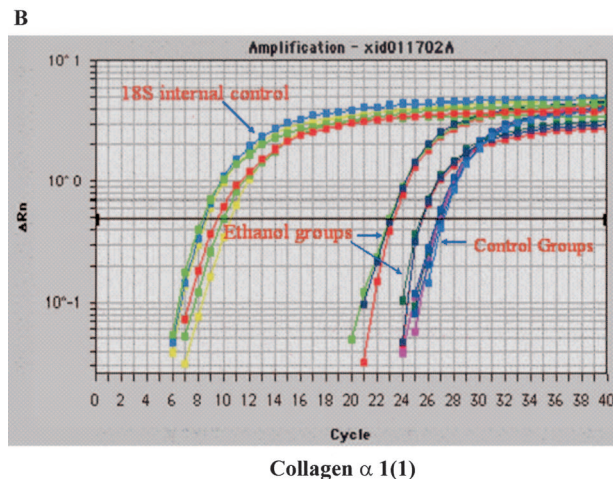
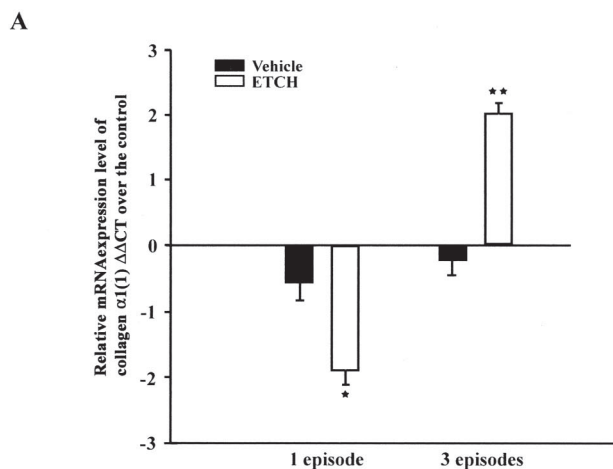


**Figure 10.** The relative mRNA expression levels of collagen- $\alpha 1(1)$  in vehicle-treated and cerulein-induced pancreatitis in both one and three episodes pancreatitis groups. **a:** The mRNA expression levels relative to the 18s RNA internal control. The bar represents the values of the mRNA expression in the ethanol-fed rats as compared to the respective control-fed rats. \*,  $P < 0.05$ ; \*\*,  $P < 0.01$ , as compared to the values in the vehicle-treated groups; **B:** the real-time amplification plots of collagen- $\alpha 1(1)$  and 18s RNA.

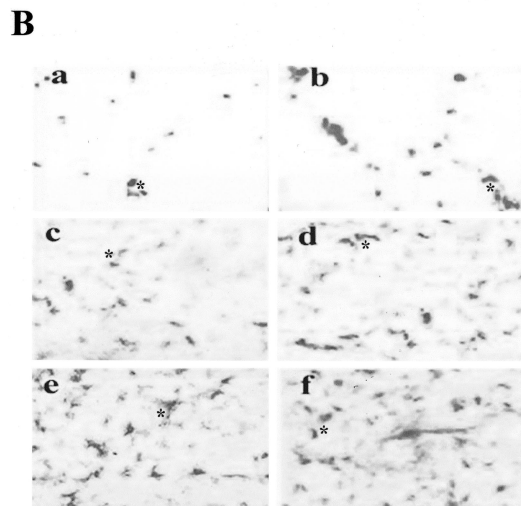
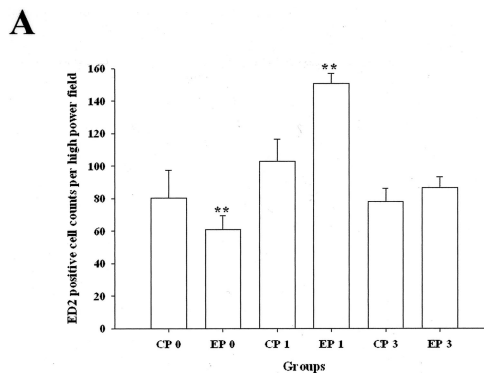


**Figure 11.** Alteration of macrophage infiltration in pancreas of control- and alcohol-fed rats. **a:** The relative changes of resident macrophages (ED2-immunoreactive positive cells) counting per high-power field in control-fed rats. \*\*,  $P < 0.01$ , as compared to the values of the corresponding control diet-fed groups. **B:** Representative tissue sections stained by ED2 immunohistochemical technique. **a:** Vehicle-treated control-fed group (CP0); **b:** vehicle-treated alcohol-fed group (EP0); **c:** 24-hours one episode of cerulein-treated control-fed rats (CP1); **d:** 24-hours one episode of cerulein-treated alcohol-fed rats (EP1); **e:** 24-hours three episodes cerulein-treated control-fed rats (CP3); and **f:** 24-hours three episodes cerulein-treated alcohol-fed rats (EP3). \*, Resident macrophages. ED2 immunohistochemical stain. Original magnifications,  $\times 100$ .

and continued alcohol exposure (eg, Figure 12). Each of these observations provides important insights into the pathogenesis of ACP.

### Inflammatory Response to Alcohol Ingestion Alone

Chronic alcohol exposure alone modestly increased serine protease mRNA expression and enzyme content as well as decreased amylase mRNA and enzyme content.<sup>43-47</sup> Chronic alcohol exposure injures the mitochondria in acinar cells, increases markers of metabolic stress, and delays pancreatic exocrine secretion.<sup>24,36,46,48</sup> Chronic alcohol exposure also alters neurohormonal control mechanisms by altering receptors, voltage-gated ion channels, and signal-transduction pathways.<sup>7</sup> Thus, chronic alcohol consumption drives metabolic and oxidative stress in acinar cells. However, alcohol at all but extreme doses does not lead to either

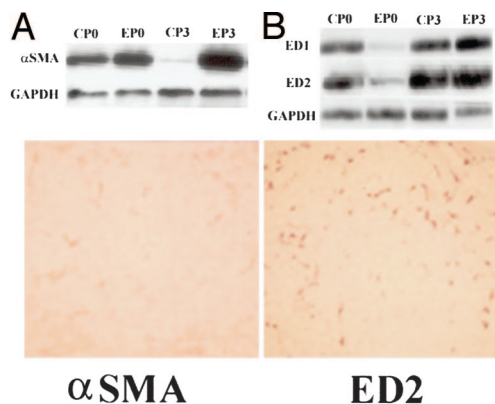


**Figure 12.** Comparison of the distribution of  $\alpha$ -SMA immune-reactive positive cells with ED2 immune-reactive positive cells in pancreas of one episode of pancreatitis in alcohol-fed rats on consecutive tissue sections at 24-hour group. **Left:**  $\alpha$ -SMA immunoblots (**top**) and  $\alpha$ -SMA immunohistochemical stain (**bottom**). **Right:** ED1 and ED2 immunoblots (**top**) and ED2 immunohistochemical stain (**bottom**).  $\alpha$ -SMA and ED2 immunohistochemical stain. Original magnifications,  $\times 100$ .

acute or chronic pancreatitis.<sup>20,40,41,49</sup> The reduction in tissue macrophage and cell number during chronic alcohol feeding likely reflects general suppression of inflammation in the naive pancreas and may explain why progression to CP is not seen without AP.

Inflammatory mechanisms are central in modulating the severity of AP and development of CP. In both human CP and experimental CP models, a series of inflammatory mediators have been identified that may play a key role in the CP process.<sup>16,50,51</sup> In ACP, T lymphocytes are frequently found in the pancreas of individual patient, with up-regulation of the MHC I and MHC II.<sup>52</sup> The T-cell population in the pancreas of patients with ACP consists of CD4<sup>+</sup> and activated CD8<sup>+</sup> cells, and to a less degree of CD56<sup>+</sup> cells.<sup>53</sup> These cells are generally cytotoxic and may lead to continual damage of the pancreas. Macrophages represent approximately another one third of the infiltrated cells in CP.<sup>50</sup> As demonstrated here, macrophage infiltration, peaked at 24 hours, and remained elevated through the subsequent experimental time points. Of note, macrophages appeared to cluster near

areas where fibrosis developed. This finding was consistent with the observation that CD68<sup>+</sup>/CCR5 cells (ie, macrophages) were prominent in the fibrotic parenchyma of pancreas in CP patients.<sup>18</sup> These macrophages appear to be active because cytokines associated with macrophage activity were up-regulated in the pancreas of CP patients. Macrophages and their role in modulating the persistence of pro- and anti-inflammatory responses, including stellate cells,<sup>54</sup> suggest that they play an important role in the development of ACP.

### Alcohol as a Susceptibility Factor for AP

*In vitro* experiments also demonstrated that pancreata isolated from rats fed alcohol for 9 to 12 months were more susceptible to cerulein-induced activation of trypsinogen and chymotrypsinogen than pancreata from the pair-fed control rats.<sup>41</sup> CCK plus ethanol could produce sixfold higher zymogen conversion than that induced by CCK alone.<sup>55</sup> In chronic alcohol-fed rats, CCK-8 infusion causes AP at concentrations lower than required for control rats.<sup>20</sup> The current study demonstrated that the severity of pancreatitis in alcohol-fed rats is greater than controls in terms of cytokine release, inflammatory cell infiltration and the activity of the macrophages, although amylase levels are similar. Together, these studies suggest that alcohol increases the risk of developing episodes of AP and contributing to severity.

### Recurrent Acute Pancreatitis Is Associated with Production of Pro- and Anti-Inflammatory Cytokines

We studied the changes in the inflammatory response to cerulein stimulation between initial episode (P1) and three-episode (P3) pancreatitis in alcohol- and control-fed rats. The proinflammatory cytokines include *macrophage inhibitory protein (MIP1 $\alpha$ )*, *tumor necrosis factor (TNF)- $\alpha$* , *monocyte chemoattractant protein (MCP-1 $\alpha$ )*, and the *cytokine regulated on activation, normal T-expressed and*

**Table 3.** Alterations of Relative Expression Levels in Alcohol-Fed Rats as Compared to Control-Fed Rats ( $\Delta\Delta$ CT: Difference of the Thresholds for PCR Amplifications in Alcohol-Fed Rats Versus Control-Fed Rats) Determined by Real-Time Quantitative PCR\*

Primer pairs	1 Episode				3 Episodes			
	3 Hour		24 Hour		3 Hour		24 Hour	
	$\Delta\Delta$ CT	P value	$\Delta\Delta$ CT	P value	$\Delta\Delta$ CT	P value	$\Delta\Delta$ CT	P value
HIF-1 $\alpha$	-0.57	0.0023	3.63	<0.0001	-0.30	0.0849	-1.11	0.0001
HIF-3 $\alpha$	-0.95	0.0519	1.80	<0.0001	0.57	0.2406	2.73	0.0001
MIP-1 $\alpha$	-0.96	0.0158	-0.14	0.5454	1.97	<0.0001	1.9	<0.0001
MCP-1 $\alpha$	-1.13	0.0024	2.36	0.0064	1.38	0.0078	1.14	0.001
RANTES	-5.73	<0.0001	-0.10	0.7571	0.53	0.0008	-0.28	0.2137
TGF- $\beta$ 1	-2.66	0.0001	4.75	0.0057	-0.32	0.1560	2.21	0.0012
IL-10	-1.13	0.0061	0.91	0.0159	-0.95	0.0024	1.24	0.0260
IL-12	-4.74	<0.0001	0.44	0.4390	-0.57	0.5867	0.77	0.0558
Collagen $\alpha$ 1(1)	-3.68	<0.0001	4.51	0.0002	-1.26	0.0005	2.80	0.0003
Procollagen $\alpha$ 2(1)	-3.12	<0.0001	3.61	0.0128	-1.12	<0.0001	3.34	<0.0001
Fibronectin	-1.42	0.0045	5.43	0.0006	-1.04	0.0005	2.70	<0.0001

\* Negative value means a down regulation of mRNA expression in pancreas of alcohol-fed rats as compared to the expression levels in those in control-fed rats.



secreted (*RANTES*). The anti-inflammatory factors include *TGF- $\beta$* , *IL-10*, and *HIF-1 $\alpha$* . A single episode of cerulein treatment in alcohol-fed rats significantly up-regulated expression of *MCP-1 $\alpha$* , *RANTES*, and *TNF- $\alpha$* . The repeated cerulein treatments in alcohol-fed rats (EP3) triggered much higher levels of *TNF- $\alpha$* , *MCP-1 $\alpha$* , and *RANTES*. The increased *TNF- $\alpha$*  level persisted even 96 hours after the final cerulein injection. The observation of continuously increased *TNF- $\alpha$*  and *MIP-1 $\alpha$*  supports a major role for active macrophages in initiating pancreatitis.

The cytokine profile in recurrent pancreatitis differs from the profile of a single episode by the up-regulation of *TGF- $\beta$*  and *IL-10*, which are potent anti-inflammatory cytokines released by macrophages. These cytokines may limit the severity of AP (decrease amylase, edema, and inflammatory cell infiltration), but drive fibrosis through acting on PSC.<sup>56,57</sup> The effect of an alcohol background on the inflammatory responses (EP3 versus CP3) was most striking with respect to *TGF- $\beta$* , *IL-10*, *MIP-1 $\alpha$* , and *HIF-3 $\alpha$*  release, as well as to the degree of macrophage infiltration. These factors are strongly linked with the marked increase in fibrosis-associated proteins seen in the EP3 rats versus other conditions.

One episode of cerulein pancreatitis in rats only transiently increased expression of *TGF- $\beta$* .<sup>58</sup> The repeated cerulein treatments in alcohol-fed rats maintained elevated *TGF- $\beta$*  throughout the experimental period at both mRNA and protein levels. The time course of the increased *TGF- $\beta$*  parallels the development of fibrosis.<sup>56,59,60</sup> When *TGF- $\beta$*  is given to mice during repeated episodes of cerulein pancreatitis, the pancreas responds with enhanced matrix deposition and fibrosis as seen in CP.<sup>26,61</sup> In the current study, repeated cerulein treatments caused a sustained elevation of *TGF- $\beta$* , although the peak levels in the subsequent acute attack decreased (in parallel with less severe proinflammatory response to injury).

### Only Alcohol Plus RAP Produce Significant Fibrosis

Pancreatic fibrosis may develop as intralobular, perilobular, and a mixture of both intralobular and perilobular fibrosis.<sup>62,63</sup> Both subtypes of fibrosis were seen in the current model with a predominance of intralobular septal fibrosis. Both trichrome and Sirius Red staining revealed the presence of collagen fibers around acinar cells, and between pancreatic lobules (Figure 5). Histological evidence paralleled increased extracellular matrix expression at mRNA and protein levels. In contrast, minimal morphological changes in the pancreas were identified in the rats fed ethanol alone, and a few changes were seen in CP1 and EP1 rats, even at 96 hours. However, with repeated cerulein treatments in alcohol-fed rats (EP3), a robust, patchy pattern of collagen deposition developed that was similar to early human ACP. Therefore, chronic alcohol feeding combined with repeated cerulein treatment results in a model of ACP that parallels the major aspects of the human disease.

### Acknowledgments

We thank the Center for Human Genetics and Integrative Biology, University of Pittsburgh, for conducting real-time quantitative PCR and scan of the microarray slides; and Dr. Christopher Hanck for his comments on the manuscript.

### References

1. Etemad B, Whitcomb DC: Chronic pancreatitis: diagnosis, classification, and new genetic developments. *Gastroenterology* 2001, 120: 682–707
2. Lankisch PG, Lowenfels AB, Maisonneuve P: What is the risk of alcoholic pancreatitis in heavy drinkers? *Pancreas* 2002, 25:411–412
3. Schneider A, Whitcomb DC, Singer MV: Animal models in alcoholic pancreatitis—what can we learn? *Pancreatol* 2002, 2:189–203
4. Gronroos JM, Aho HJ, Nevalainen TJ: Cholinergic hypothesis of alcoholic pancreatitis. *Dig Dis* 1992, 10:38–45
5. Korsten MA, Wilson JS, Haber PS: An overview of extrapancreatic factors in the pathogenesis of alcoholic pancreatitis. *Alcohol Alcohol* 1994, 2:S377–S384
6. Pitchumoni CS: Evaluation of etiological hypotheses and a study of early lesions in alcoholic pancreatitis. *Alcohol Alcohol* 1994, 2:S359–S363
7. Niebergall-Roth E, Harder H, Singer MV: A review: acute and chronic effects of ethanol and alcoholic beverages on the pancreatic exocrine secretion in vivo and in vitro. *Alcohol Clin Exp Res* 1998, 22:1570–1583
8. Kloppel G: Progression from acute to chronic pancreatitis. A pathologist's view. *Surg Clin North Am* 1999, 79:801–814
9. Ammann RW, Buehler H, Bruehlmann W, Kehl O, Muench R, Stamm B: Acute (nonprogressive) alcoholic pancreatitis: prospective longitudinal study of 144 patients with recurrent alcoholic pancreatitis. *Pancreas* 1986, 1:195–203
10. Ammann RW, Muellhaupt B, Meyenberger C, Heitz PU: Alcoholic nonprogressive chronic pancreatitis: prospective long-term study of a large cohort with alcoholic acute pancreatitis (1976–1992). *Pancreas* 1994, 9:365–373
11. Whitcomb DC, Gorry MC, Preston RA, Furey W, Sossenheimer MJ, Ulrich CD, Martin SP, Gates LK, Amann ST, Toskes PP, Liddle R, McGrath K, Uomo G, Post JC, Ehrlich GD: Hereditary pancreatitis is caused by a mutation in the cationic trypsinogen gene. *Nat Genet* 1996, 14:141–145
12. Gorry MC, Gabbaizedeh D, Furey W, Gates LK, Preston RA, Aston CE, Zhang Y, Ulrich C, Ehrlich GD, Whitcomb DC: Mutations in the cationic trypsinogen gene are associated with recurrent acute and chronic pancreatitis. *Gastroenterology* 1997, 113:1063–1068
13. Whitcomb DC: Hereditary pancreatitis: new insights into acute and chronic pancreatitis. *Gut* 1999, 45:317–322
14. Gukovskaya AS, Vaquero E, Zaninovic V, Gorelick FS, Lusic AJ, Brennan ML, Holland S, Pandolfi SJ: Neutrophils and NADPH oxidase mediate intrapancreatic trypsin activation in murine experimental acute pancreatitis. *Gastroenterology* 2002, 122:974–984
15. Demols A, Le Moine O, Desalle F, Quertinmont E, Van Laethem JL, Deviere J: CD4(+)T cells play an important role in acute experimental pancreatitis in mice. *Gastroenterology* 2000, 118:582–590
16. Ockenga J, Jacobs R, Kemper A, Benschop RJ, Schmidt RE, Manns MP: Lymphocyte subsets and cellular immunity in patients with chronic pancreatitis. *Digestion* 2000, 62:14–21
17. Hanck C, Rossol S, Singer MV: Immunological changes of mild acute pancreatitis in late-stage alcoholic chronic pancreatitis. *Dig Dis Sci* 1999, 44:1768–1773
18. Goecke H, Forssmann U, Ugucconci M, Friess H, Conejo-Garcia JR, Zimmermann A, Baggiolini M, Buchler MW: Macrophages infiltrating the tissue in chronic pancreatitis express the chemokine receptor CCR5. *Surgery* 2000, 128:806–814
19. Koko V, Todorovic V, Nikolic JA, Glisic R, Cacic M, Lackovic V, Petronijevic L, Stojkovic M, Varagic J, Janic B: Rat pancreatic B-cells after chronic alcohol feeding. A morphometric and fine structural study. *Histol Histopathol* 1995, 10:325–337

20. Pandol SJ, Periskic S, Gukovsky I, Zaninovic V, Jung Y, Zong Y, Solomon TE, Gukovskaya AS, Tsukamoto H: Ethanol diet increases the sensitivity of rats to pancreatitis induced by cholecystokinin octapeptide. *Gastroenterology* 1999, 117:706–716
21. Tsukamoto H, Townner SJ, Yu GS, French SW: Potentiation of ethanol-induced pancreatic injury by dietary fat. Induction of chronic pancreatitis by alcohol in rats. *Am J Pathol* 1988, 131:246–257
22. Li HS, Zhang JY, Thompson BS, Deng XY, Ford ME, Wood PG, Stolz DB, Eagon PK, Whitcomb DC: Rat mitochondrial ATP synthase ATP5G3: cloning and upregulation in pancreas after chronic ethanol feeding. *Physiol Genomics* 2001, 6:91–98
23. Norton ID, Apte MV, Lux O, Haber PS, Pirola RC, Wilson JS: Chronic ethanol administration causes oxidative stress in the rat pancreas. *J Lab Clin Med* 1998, 131:442–446
24. Deng X, Wood PG, Eagon PK, Whitcomb DC: Chronic alcohol ingestion alters neurohormonal control of the rat pancreas. *Pancreas* 1997, 15:432
25. Lampel M, Kern HF: Acute interstitial pancreatitis in the rat induced by excessive doses of a pancreatic secretagogue. *Virchows Arch A, Pathological Anat Histol* 1977, 373:97–117
26. Van Laethem JL, Robberecht P, Resibois A, Deviere J: Transforming growth factor beta promotes development of fibrosis after repeated courses of acute pancreatitis in mice. *Gastroenterology* 1996, 110:576–582
27. Lieber CS, DeCarli LM: Liquid diet technique of ethanol administration: 1989 update. *Alcohol Alcohol* 1989, 24:197–211
28. Deng X, Wood PG, Eagon PK, Whitcomb DC: Rapid adaptation of pancreatic exocrine function to short term alcohol feeding in rats. *Pancreatol* (in press)
29. Jung DH: Preparation and application of procion yellow starch for amylase assay. *Clin Chem Acta* 1980, 100:7–10
30. Kalf J, Schwarz NT, Walgenbach KJ, Schraut WH, Bauer AJ: Leukocytes of the intestinal muscularis: their phenotype and isolation. *J Leukocyte Biol* 1998, 63:683–691
31. Woessner Jr JF: The determination of hydroxyproline in tissue and protein samples containing small proportions of imino acids. *Arch Biochem Biophys* 1961, 93:440–447
32. Lowry OH, Rosebrough NJ, Farr AL, Randall RJ: Protein measurement with the Folin phenol reagent. *J Biol Chem* 1951, 193:265–275
33. Nieto N, Friedman SL, Greenwel P, Cederbaum AI: CYP2E1-mediated oxidative stress induces collagen type I expression in rat hepatic stellate cells. *Hepatology* 1999, 30:987–996
34. Strowski MZ, Sparmann G, Weber H, Fiedler F, Printz H, Jonas L, Goke B, Wagner AC: Caerulein pancreatitis increases mRNA but reduces protein levels of rat pancreatic heat shock proteins. *Am J Physiol* 1997, 273:G937–G945
35. Li H, Zhang J, Deng X, Thompson BS, Wood PG, Eagon PK, Whitcomb DC: Altered pancreatic gene expression in alcohol-fed rats using microarray analysis of stress and detoxification genes. *Gastroenterology* 2001, 120:A33
36. Li HS, Deng XY, Thompson BS, Zhang JY, Wood PG, Eagon PK, Whitcomb DC: Chronic ethanol consumption induces gene expression of pancreatic monitor peptide, but not SPINK1/PSTI-56, in rats. *Pancreas* 2001, 23:117–124
37. Deng X, Elm MS, Eagon PK, Whitcomb DC: Altered expression of M3 and CCK-A receptors in pancreas with alcohol and cerulein hyperstimulation. *Pancreas* 2002, 25:425
38. Singh M, LaSure MM, Bockman DE: Pancreatic acinar cell function and morphology in rats chronically fed an ethanol diet. *Gastroenterology* 1982, 82:425–434
39. Deng X, Wood PG, Eagon PK, Whitcomb DC: Chronic alcohol-induced alterations in the pancreatic secretory control mechanisms. *Dig Dis Sci* 2004, 45:805–819
40. Gronroos JM, Aho HJ, Nevalainen TJ: Effects of chronic alcohol intake and secretory stimulation on sodium taurocholate-induced pancreatic necrosis in the rat. *J Surg Res* 1989, 47:360–364
41. Ponnappa BC, Marciniak R, Schneider T, Hoek JB, Rubin E: Ethanol consumption and susceptibility of the pancreas to cerulein-induced pancreatitis. *Pancreas* 1997, 14:150–157
42. Schneider A, Whitcomb DC: Hereditary pancreatitis: a model for inflammatory diseases of the pancreas. *Best Practice Res Clin Gastroenterol* 2002, 16:347–363
43. Steer ML, Glazer G, Manabe T: Direct effects of ethanol on exocrine secretion from the in vitro rabbit pancreas. *Dig Dis Sci* 1979, 24:769–774
44. Perkins PS, Rutherford RE, Pandol SJ: Effect of chronic ethanol feeding on digestive enzyme synthesis and mRNA content in rat pancreas. *Pancreas* 1995, 10:14–21
45. Apte M, Norton I, Haber P, Applegate T, Korsten M, McCaughan G, Pirola R, Wilson J: The effect of ethanol on pancreatic enzymes—a dietary artifact? *Biochim Biophys Acta* 1998, 1379:314–324
46. Schmidt DN, Pandol SJ: Differing effects of ethanol on in vitro stimulated pancreatic enzyme secretion in ethanol-fed and control rats. *Pancreas* 1990, 5:27–36
47. Solomon N, Solomon TE, Jacobson ED, Shanbour LL: Direct effects of alcohol on in vivo and in vitro exocrine pancreatic secretion and metabolism. *Am J Dig Dis* 1974, 19:253–260
48. Hirano H, Shimosegawa T, Meguro T, Shiga N, Koizumi M, Toyota T: Effects of ethanol on meal-stimulated secretion of pancreatic polypeptide and cholecystokinin: comparison of healthy volunteers, heavy drinkers, and patients with chronic pancreatitis. *J Gastroenterol* 1996, 31:86–93
49. Kono H, Nakagami M, Rusyn I, Connor HD, Stefanovic B, Brenner DA, Mason RP, Arteel GE, Thurman RG: Development of an animal model of chronic alcohol-induced pancreatitis in the rat. *Am J Physiol* 2001, 280:G1178–G1186
50. Emmrich J, Weber I, Nausch M, Sparmann G, Koch K, Seyfarth M, Lohr M, Liebe S: Immunohistochemical characterization of the pancreatic cellular infiltrate in normal pancreas, chronic pancreatitis and pancreatic carcinoma. *Digestion* 1998, 59:192–198
51. Sparmann G, Behrend S, Merkord J, Kleine HD, Graser E, Ritter T, Liebe S, Emmrich J: Cytokine mRNA levels and lymphocyte infiltration in pancreatic tissue during experimental chronic pancreatitis induced by dibutyltin dichloride. *Dig Dis Sci* 2001, 46:1647–1656
52. Cavallini G, Frulloni L: Autoimmunity and chronic pancreatitis: a concealed relationship. *J Pancreas* 2001, 2:61–68
53. Hunger RE, Mueller C, Z'Graggen K, Friess H, Buchler MW: Cytotoxic cells are activated in cellular infiltrates of alcoholic chronic pancreatitis. *Gastroenterology* 1997, 112:1656–1663
54. Apte MV, Haber PS, Darby SJ, Rodgers SC, McCaughan GW, Korsten MA, Pirola RC, Wilson JS: Pancreatic stellate cells are activated by proinflammatory cytokines: implications for pancreatic fibrogenesis. *Gut* 1999, 44:534–541
55. Katz M, Carangelo R, Miller LJ, Gorelick F: Effect of ethanol on cholecystokinin-stimulated zymogen conversion in pancreatic acinar cells. *Am J Physiol* 1996, 270:G171–G175
56. Muller-Pillasch F, Menke A, Yamaguchi H, Elsasser HP, Bachem M, Adler G, Gress TM: TGFbeta and the extracellular matrix in pancreatitis. *Hepato-Gastroenterol* 1999, 46:2751–2756
57. Rongione AJ, Kusske AM, Kwan K, Ashley SW, Reber HA, McFadden DW: Interleukin 10 reduces the severity of acute pancreatitis in rats. *Gastroenterology* 1997, 112:960–967
58. Riesel E, Friess H, Zhao L, Wagner M, Uhl W, Baczako K, Gold LI, Korc M, Buchler MW: Increased expression of transforming growth factor beta s after acute oedematous pancreatitis in rats suggests a role in pancreatic repair. *Gut* 1997, 40:73–79
59. Kato Y, Inoue H, Fujiyama Y, Bamba T: Morphological identification of and collagen synthesis by periacinar fibroblastoid cells cultured from isolated rat pancreatic acini. *J Gastroenterol* 1996, 31:565–571
60. Apte MV, Haber PS, Applegate TL, Norton ID, McCaughan GW, Korsten MA, Pirola RC, Wilson JS: Periacinar stellate shaped cells in rat pancreas: identification, isolation, and culture. *Gut* 1998, 43:128–133
61. Menke A, Yamaguchi H, Gress TM, Adler G: Extracellular matrix is reduced by inhibition of transforming growth factor beta1 in pancreatitis in the rat. *Gastroenterology* 1997, 113:295–303
62. Kennedy RH, Bockman DE, Uscanga L, Choux R, Grimaud JA, Sarles H: Pancreatic extracellular matrix alterations in chronic pancreatitis. *Pancreas* 1987, 2:61–72
63. Ammann RW, Heitz PU, Kloppel G: The “two-hit” pathogenetic concept of chronic pancreatitis. *Int J Pancreatol* 1999, 25:251